Article

Quantum Dot Fluorescence Quenching Pathways with Cr(III) Complexes. Photosensitized NO Production from *trans*-Cr(cyclam)(ONO)

Daniel Neuman, Alexis D. Ostrowski, Alexander A. Mikhailovsky, Ryan O. Absalonson, Geoffrey F. Strouse, and Peter C. Ford

J. Am. Chem. Soc., **2008**, 130 (1), 168-175 • DOI: 10.1021/ja074164s

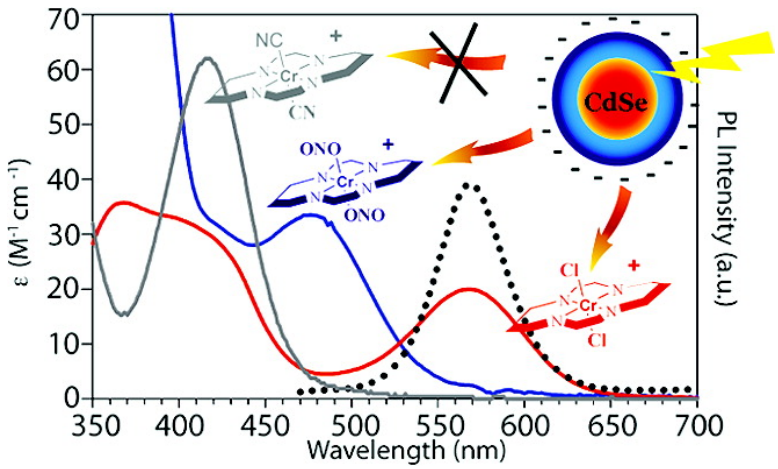

More About This Article

Additional resources and features associated with this article are available within the HTML version:

- Supporting Information
- Links to the 2 articles that cite this article, as of the time of this article download
- Access to high resolution figures
- Links to articles and content related to this article
- Copyright permission to reproduce figures and/or text from this article

View the Full Text HTML

J|A|C|S
ARTICLES
Published on Web 12/13/2007

Quantum Dot Fluorescence Quenching Pathways with Cr(III) Complexes. Photosensitized NO Production from *trans*-Cr(cyclam)$(ONO)_2^+$

Daniel Neuman,[†,#] Alexis D. Ostrowski,[†] Alexander A. Mikhailovsky,[†] Ryan O. Absalonson,[†] Geoffrey F. Strouse,[‡] and Peter C. Ford*[,†]

Department of Chemistry and Biochemistry, University of California, Santa Barbara, Santa Barbara, California 93106-9510, and Department of Chemistry and Biochemistry, Florida State University, Tallahassee, Florida 32306-4390

Received June 7, 2007; E-mail: Ford@chem.ucsb.edu

Abstract: Described is the photoluminescence (PL) of water-soluble CdSe/ZnS core/shell quantum dots (QDs) as perturbed by salts of the chromium(III) complexes *trans*-Cr(cyclam)Cl_2^+ (**1**), *trans*-Cr(cyclam)-$(ONO)_2^+$ (**2**), and *trans*-Cr(cyclam)$(CN)_2^+$ (**3**) (cyclam = 1,4,8,11-tetraazacyclo-tetradecane). The purpose is to probe the characteristics of such QDs as antennae for photosensitized release of bioactive agents (in the present case, the bioregulatory molecule NO) from transition metal centers. Addition of **1** or **2** to a QD solution results in concentration-dependent quenching of the band edge emission, but **3** has a minimal effect. Added KCl strongly attenuates the quenching by **1**, and this suggests that the Cr(III) cations and the QDs form electrostatic assemblies via ion pairing on the negatively charged QD surfaces. Quenching by **2**, a known photochemical NO precursor, was accompanied by photosensitized NO release. All three, however, do quench the broad red emission (~650−850 nm) attributed to radiative decay of surface trapped carriers. The effect of various concentrations of **1** on time-resolved PL and absorbance were explored using ultrafast spectroscopic methods. These observations are interpreted in terms of the Förster resonance energy-transfer mechanism for quenching of the band edge PL by multiple units of **1** or **2** at the QD surface, whereas quenching of the low-energy trap emission occurs via a charge-transfer pathway.

Introduction

Nitric oxide (NO) has key regulatory roles in mammalian biology, and there is considerable interest in designing compounds for controlled delivery to physiological targets.[1] In this context, our laboratory[2,3] and others[4] have been concerned with developing transition metal complexes for photoactivated NO delivery to specific tissues upon demand. However, the low absorptivity of many such photochemical NO precursors at the longer visible wavelengths where tissue penetration is greater[5] may limit their utility. To address this problem, we have initiated studies with strongly absorbing antennae to increase light harvesting capability and to enhance the rate of photochemical NO release.[3c]

Semiconductor quantum dots (QDs) are attractive for this application due to the strong visible absorption for the exciton,[6] the large two photon absorption cross-sections,[7] the ease of tunability that allows optimizing energy overlap, and the simplicity of modifications to allow attachment of desired molecules at the surface of the nanocrystal, and/or to impart water solubility or biological specificity.[8,9] Quantum confinement effects allow

[†] University of California.
[‡] Florida State University.
[#] Present address: Wellman Laboratories for Photomedicine, Thier 224, Harvard Medical School, Massachusetts General Hospital, Boston, Massachusetts 02114.

(1) (a) Saavedra, J. E.; Hoffman, A.; Bove, A. A.; Isaac, L.; Hrabie, J. A.; Keefer, L. K. *J. Med. Chem.* **1991**, *34*, 3242−3247. (b) Wang, P. G.; Xian, M.; Tang, X.; Wu, X.; Wen, Z.; Cai, T.; Janczuk, A. J. *Chem. Rev.* **2002**, *102*, 1091−1134. (c) King, S. B. *Curr. Top. Med. Chem.* **2005**, *5*, 665−673. (d) Wheatley, P.; Butler, A. R.; Crane, M.; Fox, S.; Xiao, B.; Rossi, A.; Megson, I. L.; Morris, R. E. *J. Am. Chem. Soc.* **2006**, *128*, 502−509.
(2) (a) Bourassa, J.; DeGraff, W.; Kudo, S.; Wink, D. A.; Mitchell, J. B.; Ford, P. C. *J. Am. Chem. Soc.* **1997**, *119*, 2853−2860. (b) Ford, P. C.; Bourassa, J.; Miranda, K. M.; Lee, B.; Lorkovic, I.; Boggs, S.; Kudo, S.; Laverman, L. *Coord. Chem. Rev.* **1998**, *171*, 185−202. (c) Works, C. F.; Ford, P. C. *J. Am. Chem. Soc.* **2000**, *122*, 7592−7593 (d) Wecksler, S.; Mikhailovsky, A.; Ford, P. C. *J. Am. Chem. Soc.* **2004**, *126*, 13566−13567. (e) Wecksler, S. R.; Mikhailovsky, A.; Korystov, D.; Ford, P. C. *J. Am. Chem. Soc.* **2006**, *128*, 3831−3837.
(3) (a) DeLeo, M. A.; Ford, P. C. *J. Am. Chem. Soc.* **1999**, *121*, 1980−1981. (b) DeLeo, M. A.; Ford, P. C. *Coord. Chem. Rev.* **2000**, *208*, 47−59. (c) DeRosa, F.; Bu, X.; Ford, P. C. *Inorg. Chem.* **2005**, *44*, 4157−4165. (d) Ford, P. C. *Acct. Chem. Res.* in press.
(4) (a) Tfouni, E.; Krieger, M.; McGarvey, B. R.; Franco, D. W. *Coord. Chem. Rev.* **2003**, *236*, 57−69. (b) Pavlos, C. M.; Xu, H.; Toscano, J. P. *Curr. Top. Med. Chem.* **2005**, *5*, 635−645. (c) Eroy-Reveles, A A.; Leung, Y.; Mascharak, P. K. *J. Am. Chem. Soc.* **2006**, *128*, 7166−7167.
(5) (a) Dougherty, T. J; Marcus, S. L. *Eur. J. Cancer* **1992**, *28A*, 1734−42. (b) Konig, K. *J. Microscopy* **2000**, *200*, 83−104.
(6) (a) Leatherdale, C. A.; Woo, W.-K.; Mikulec, F. V.; Bawendi, M. G. *J. Phys. Chem. B* **2002**, *106*, 7619−7622. (b) Schmelz, O.; Mews, A.; Basché, T.; Herrmann, A.; Müllen, K. *Langmuir* **2001**, *17*, 2861−2865. (c) Yu, W. W.; Qu, L.; Guo, W.; Peng, X. *Chem. Mater.* **2003**, *15*, 2854−2860.
(7) Larson Daniel, R.; Zipfel, W. R.; Williams, R. M.; Clark, S. W.; Bruchez, M. P.; Wise, F. W.; Webb, W. W. *Science* **2003**, *300*, 1434−1436.
(8) Mattoussi, H.; Mauro, J. M.; Goldman, E. R.; Anderson, G. P.; Sundar, V. C.; Mikulec, F. V.; Bawendi, M. G. *J. Am. Chem. Soc.* **2000**, *122*, 12142−12150.
(9) (a) Pinaud, F.; Michalet, X.; Bentolila, L. A.; Tsay, J. M.; Doose, S.; Li, J. J.; Iyer, G.; Weiss, S. *Biomatererials* **2006**, *27*, 1679−1687. (b) Alivisatos, A. P.; Gu, W.; Larabell, C. *Annu. Rev. Biomed. Eng.* **2005**, *7*, 55−76. (c) Gao, X.; Yang, L.; Petros, J. A.; Marshall, F. F.; Simons, J. W.; Nie, S. *Curr. Opin. Biotech.* **2005**, *16*, 63−72. (d) Medintz, I. L.; Tetsuo Uyeda, H.; Goldman, E. R.; Mattoussi, H. *Nat. Mater.* **2005**, *4*, 435−446.

10.1021/ja074164s CCC: $40.75

one to shift the QD optical absorbance and photoluminescence (PL) by varying the size,[10] suggesting that QDs should be tunable antennae for photoreaction sensitization. Notably, QDs have proved effective for several such applications[11−13] including singlet oxygen production.[12] Although there have been reports of nanoparticles[14] as devices for thermally activated NO delivery, the use of semiconductor QDs to photosensitize NO release from stable precursors has not been addressed except in a recent communication from this laboratory.[15]

Here, we describe studies that probe energy-transfer processes between water-soluble core/shell CdSe/ZnS quantum dots and several transition metal complexes. These studies were initiated with the goal of providing guidelines for the design of systems where QD photooptical properties facilitate the photochemical release of NO or other bioactive agent from a transition metal precursor. Aqueous solubility of the QDs was accomplished by exchanging surface capping groups with dihydrolipoic acid (which is ionized in moderately alkaline media),[8] and we have probed the photoluminescence behavior of water-soluble CdSe/ZnS core/shell QDs in buffer solutions as affected by the Cr(III) complexes *trans*-$Cr(cyclam)Cl_2^+$ (**1,** Cl^- salt), *trans*-$Cr(cyclam)(ONO)_2^+$ (**2,** BF_4^- salt), or *trans*-$Cr(cyclam)(CN)_2^+$ (**3**, ClO_4^- salt).[3] The time-resolved PL and the temporal excited-state absorption behavior of the negatively charged QDs were monitored at various concentrations of added **1**, **2**, or **3**. These studies indicate that the donor−acceptor interaction in solution is dominated by preassociation between the anionic CdSe/ZnS QDs and the cationic Cr(III) complexes prior to optical excitation. The photophysical and photochemical consequences of such interactions are described and discussed.

Experimental Section

Synthesis of Water Soluble CdSe/ZnS Core/Shell QDs. A three-step procedure preparing the CdSe cores by pyrolysis of organometallic precursors, growing ZnS shells around the cores, and exchanging DHLA for the surface ligands[8] was used for the synthesis of water-soluble core/shell QDs.

The CdSe cores were prepared by decomposition of dimethylcadmium (Me_2Cd) and trioctylphosphine selenide (TOP−Se) in a 40:20:40 (mol %) melt of hexadecylamine (HDA), trioctylphosphine (TOP), and trioctylphosphine oxide (TOPO) according to published procedures.[16] After several purification steps (see Supporting Information), the QDs were dissolved in a solution of ∼0.1 M HDA in hexanes, and their size and concentration were estimated by correlating the peak position and intensity of the lowest exciton transition ($1S-1S_{3/2}$) with the reported QD sizing curve[17] and the size dependent extinction coefficient[6c] of this transition. This preparation gave ∼2.4 μmol of CdSe cores with a lowest excitonic transition centered at 541 nm and a narrow photoluminescence (full width at half-maximum (fwhm = 29 nm) centered at 555 nm (see Supporting Information Figure S1). On the basis of the position of the $1S-1S_{3/2}$ absorption band, these CdSe core QDs have diameters of ∼3.8 nm.[17] The PL quantum yield (Φ_{PL}) was 11%.

A zinc sulfide shell was grown on the cores using established procedures[18] with quantities of the precursors (diethylzinc and hexamethyldisilathiane) necessary to give a six monolayer thick shell calculated from the core size and the bulk lattice parameters of CdSe and ZnS. The resulting core/shell QDs were stored in the dark in their growth mixture. Isolation/purification was affected by flocculation of the QDs with four volume equivalents of methanol. Following supernatant removal, the QDs were washed twice with methanol and dried under reduced pressure. These procedures gave core/shell QDs with a PL band centered at 561 nm (fwhm = 45 nm) and Φ_{PL} of ∼15%.

The HDA/TOP/TOPO surface ligands were exchanged for dihydrolipoic acid (DHLA) (freshly prepared by the reduction of lipoic acid with sodium borohydride[19]) according to published procedures with slight modifications (see Supporting Information).[8,20] Following purification, the DHLA capped core/shell QDs had a PL maximum centered at 570 nm (fwhm = 45 nm) and a Φ_{PL} of ∼2% in 15 mM phosphate buffer solution at pH 8.2.

Synthesis of Chromium(III) Complexes. *trans*-$[Cr(cyclam)Cl_2]Cl$ (**1**) was prepared according to Bakac and Espenson[21] and twice recrystallized from hot aq. HCl (1 M). UV−vis (H_2O): λ_{max} in nm (ϵ in $M^{-1}\,cm^{-1}$): 368 (27.1), 404sh (24.3), 570 (16.9)). *trans*-$[Cr(cyclam)(ONO)_2]BF_4$ (**2**) was prepared from ***1*** in 60% yield according to DeLeo et al.[22] UV−vis (H_2O): 340 (246), 476 (32). *trans*-$[Cr(cyclam)(CN)_2]ClO_4$ (**3**) was prepared from **1** according to Kane-Maguire et al.[23] UV−vis (H_2O): 328 (54), 414(62).

Luminescence Quantum Yield and Quenching Experiments. All photophysical experiments with the water-soluble QDs were carried out in 15 mM phosphate buffer solution at pH 8.2. Photoluminescence spectra and intensities under continuous excitation were measured in a right angle configuration on a SPEX Fluorolog−2 spectrofluorimeter. The resolution was ∼4 nm unless otherwise indicated. Absorption spectra were recorded on a Shimadzu Model UV-2401 spectrophotometer.

Samples used to determine the PL quantum yield of the water-soluble core/shell QDs were excited at 450 nm in a 10 mm path length quartz cuvette. The emission intensities were compared quantitatively to an absorbance matched solution of $[Ru(bpy)_3](PF_6)_2$ (bpy = 2,2′-bipyridine) in degassed acetonitrile (Φ_{PL} = 0.062).[24]

Quenching experiments were carried out in pH 8.2 buffer solution. Samples of QDs or mixtures of QDs and varying concentrations of **1**, **2**, or **3** were entrained with Ar to remove O_2. Measurements were taken

(10) Alivisatos, A. P. *J. Phys. Chem.* **1996**, *100*, 13226−13239.
(11) (a) Wijtmans, M.; Rosenthal, S. J.; Zwanenburg, B.; Porter, N. A *J. Am. Chem. Soc.* **2006**, *128*, 11720−11726. (b) Warrier, M.; Lo, M. K. F.; Monbouquette, H.; Garcia-Garibay, *M. A. Photochem. Photobiol. Sci.* **2004**, *3*, 859−863.
(12) (a) Samia, A. C. S.; Chen, X.; Burda, C. *J. Am. Chem. Soc.* **2003**, *125*, 15736−15737. (b) Shi, L.; Hernandez, B.; Selke, M. *J. Am. Chem. Soc.* **2006**, *128*, 6278−6279. (c) Clarke, S.; Hollmann, C. A.; Zhang, Z.; Suffern, D.; Bradforth, S. E.; Dimitrijevic, N. M.; Minarik, W. G.; Nadeau, J. L. *Nat. Mater.* **2006**, *5*, 409−417. (d) Bakalova, R.; Ohba, H.; Zhelev, Z.; Nagase, T.; Jose, R.; Ishikawa, M.; Baba, Y. *Nano Lett.* **2004**, *4*, 1567−1573. (e) Dayal, S.; Krolicki, R.; Burda, C. *Proc. SPIE* **2005**, *5705*, 247−254. (f) Shi, L.; Hernandez, B.; Selke, M. *J. Am. Chem. Soc.* **2006**, *128*, 6278−6279.
(13) (a) Sykora, M.; Petruska, M. A.; Alstrum-Acevedo, J.; Bezel, I.; Meyer, T. J.; Klimov, V. I. *J. Am. Chem. Soc.* **2006**, *128*, 9984−9985. (b) Sharma, S. N.; Pillai, Z.; Kamat, P. V. *J. Phys. Chem. B* **2003**, *107*, 10088−10093. (c) Landes, C.; Burda, C.; Braun, M.; El-Sayed, M. A. *J. Phys. Chem. B* **2001**, *105*, 2981−2986.
(14) (a) Rothrock, A. R.; Donkers, R. L.; Schoenfisch, M. H. *J. Am. Chem. Soc.* **2005**, *127*, 9362−9363. (b) Caruso, E. B.; Petralia, S.; Conoci, S.; Giuffrida, S.; Sortino, S. *J. Am. Chem. Soc.* **2007**, *129*, 480−481.
(15) Neuman, D.; Ostrowski, A. D.; Absalonson, R. O.; Strouse, G. F.; Ford, P. C. *J. Am. Chem. Soc.* **2007**, *129*, 4146−4147.
(16) (a) Murray, C. B.; Norris, D. J.; Bawendi, M. G. *J. Am. Chem. Soc.* **1993**, *115*, 8706−8715. (b) Talapin, D. V.; Rogach, a. L.; Kornowski, A.; Haase, M.; Weller, H. *Nano Lett.* **2001**, *1*, 207−211. (c) de Mello, Donega, C.; Hickey, S. G.; Wuister, S.; Vanmaekelbergh, D.; Meijerink, A. *J. Phys. Chem. B* **2003**, *107*, 489−496.
(17) Mikulec, F. V.; Kuno, M.; Bennati, M.; Hall, D. A.; Griffin, R. G.; Bawendi, M. G. *J. Am. Chem. Soc.* **2000**, *122*, 2532−2540.
(18) Dabbousi, B. O.; Rodriguez-Viejo, J.; Mikulec, F. V.; Heine, J. R.; Mattoussi, H.; Ober, R.; Jensen, K. F.; Bawendi, M. G. *J. Phys. Chem. B* **1997**, *101*, 9463−9475.
(19) (a) Uyeda, H. T.; Medintz, I. L.; Jaiswai, J. K.; Simon, S. M.; Mattoussi, H. *J. Am. Chem. Soc.* **2005**, *127*, 3870−3878. (b) Gunsalus, I. C.; Barton, L. S.; Gruber, W. *J. Am. Chem. Soc.* **1956**, *78*, 1763−1766. (c) Wagner, A. F.; Walton, E.; Boxer, G. E.; Pruss, M. P.; Holly, F. W.; Folkers, K. *J. Am. Chem. Soc.* **1956**, *78*, 5079−5081.
(20) Cheng, C.-T.; Chen, C.-Y.; Lai, C.- W.; Liu, W.- H.; Pu, S.- C.; Chou, P.- T.; Chou, Y.- H.; Chiu, H.-T. *J. Mater. Chem.* **2005**, *15*, 3409−3414.
(21) Bakac, A.; Espenson, J. H. *Inorg. Chem.* **1992**, *31*, 1108−1109.
(22) De Leo, M. A.; Bu, X.; Bentow, J.; Ford, P. C. *Inorg. Chim. Acta* **2000**, *300−302*, 944−950.
(23) Kane-Maguire, N. A. P.; Bennett, J. A.; Miller, P. K. *Inorg. Chim. Acta* **1983**, *76*, L123−L125.
(24) Caspar, J. V.; Meyer, T. J. *J. Am. Chem. Soc.* **1983**, *105*, 5583−5590.

in 10 mm cuvettes immediately after dilution. In mixtures with **1** or **3**, samples were excited at 460 nm in a region of relatively low absorbance of the added Cr(III) salt to avoid inner-filter effects. For experiments with **2**, samples were excited at 366, 460, or 546 nm, and the PL spectra were corrected for absorbance due to the chromium complex.

Luminescence Lifetime Measurements. These were performed in the UCSB Optical Characterization Facility using the time-correlated single-photon-counting technique (TCSPC).[25] The sample was excited by 460 nm laser pulses (~120 fs, <1 nJ) produced via the second harmonic generation of the output from a Ti:sapphire laser (Spectra-Physics Tsunami). To avoid saturation of the chromophore, the repetition rate of the excitation pulses was reduced to 2 MHz by a custom-built acousto-optical pulse picker. The luminescence was dispersed in a monochromator (Acton Research SPC-300) and detected by a micro channel-plate photomultiplier tube (MCP PMT; Hamamatsu R3809U-51). The triggering signal for the correlator board was generated by a fast photodiode illuminated via a beam splitter introduced into the excitation beam. The MCP PMT output and triggering signal were connected to a SPC-630 time-correlated single photon counting board (Becker and Hickl) that performed statistical analysis of the photon flux and restored the fluorescence transients. The instrument response function (IRF) width was found to be ~55 ps by measurements with suspensions of nonfluorescent scatterers and the detector set at a wavelength close to the excitation wavelength. No fluorescence or scattering signal was seen for solutions of the QDs when the detector monochromator was set at a wavelength outside the PL band and more than 5 nm from the excitation wavelength. The TCSPC data were not deconvoluted with IRF.

Transient Absorbance (TA) Experiments. Femtosecond TA experiments were performed in the UCSB Optical Characterization Facility with a transient absorption spectrometer similar to that described by Klimov and McBranch.[26] The system utilizes a Ti:Sapphire regenerative amplifier (SpectraPhysics Spitfire) producing 100 fs optical pulses (1 kHz repetition rate, 800 nm central wavelength pulse energy <1 mJ) from which 400 nm pulses were prepared by second harmonic generation in a 1 mm thick β-BBO crystal for excitation of the sample. The pulse energy was adjusted by a calibrated neutral density filter wheel to ensure a QD excitation level <1 exciton per nanoparticle on average. Photoinduced absorption changes were monitored by fs continuum pulses generated by focusing low energy (<2 μJ) 800 nm pulses onto a 2 mm thick crystalline sapphire plate. The delay between pump and probe pulses was varied by a translation stage with a corner cube reflector inserted into the pump beam. An optical chopper synchronized with the laser repetition frequency was employed to modulate the excitation beam and provided a synchronization signal for the lock-in amplifier (SRS SR830). Solutions of QDs or mixtures of QDs with varied concentrations of **1** were placed in 1 mm path length quartz cuvettes and entrained with Ar to remove O_2. The pump and probe beams were focused on the sample in a near-collinear geometry using a lens and a parabolic mirror, respectively. The probe light was dispersed by a monochromator (Acton SpectraPro 300) and detected by a silicon photodiode connected to a lock-in amplifier via a transimpedance amplifier. The operation of the setup was controlled by a LabView program running on a PC.

Continuous Photolysis and Nitric Oxide Detection. A NO-sensitive electrode (amiNO−700, Innovative Instruments, Inc.) was used for real-time detection of NO produced by photochemical decomposition of **2**. All experiments were done under aerated conditions in pH 8.2 buffer solution. The electrode was polarized overnight in deionized H_2O prior to use and then was allowed to equilibrate in the stirred buffer solution for ~10 min in the dark. The light (output of a high-pressure Hg arc lamp spectrally selected by band-pass filter) was turned on, taking care to ensure the electrode was not directly illuminated. Once the background signal was stable, an aliquot of **2** was added and the electrode response was monitored to determine NO release from **2** alone. Alternatively, an aliquot of QDs was introduced and allowed to mix for ~100−200 s followed by an aliquot of **2**, and the electrode response was monitored to determine NO release from the mixture.

Cyclic Voltammetry. Cyclic voltammograms were collected using a Bioanalytical Systems Electrochemical Analyzer (Model 100A) with a glassy carbon working electrode (BAS), platinum wire counter electrode, and Ag/AgCl reference electrode (BAS) in solutions of degassed acetonitrile with 0.5 M $[NBu_4]PF_6$ for the supporting electrolyte.

Results and Discussion

This report is concerned with analyzing the effects of the Cr(III) cations *trans*-Cr(cyclam)X_2^+ on the photophysical behavior of water-soluble CdSe/ZnS core/shell QDs. The goal is to evaluate the nature of energy-transfer processes that might be utilized to sensitize the photochemical release of NO (or other bioactive agents) from appropriate precursors. Neither the dichloro complex **1** ($X^- = Cl^-$)[27] nor its dicyano analog **3** show significant photoreactivity when directly excited in solution, in contrast to the dinitrito complex **2** ($X^- = ONO^-$), which releases NO with high quantum yields under similar conditions.[3a,b] Although **2** is photoactive, the Laporte forbidden, visible range, absorption bands are quite weak, so one goal of the present study is to examine the use of QDs as strongly absorbing antennae.

Figure 1 displays the absorption behavior of these three Cr(III) complexes in aqueous solution and the PL spectrum of the water-soluble QDs under analogous conditions. For **1**, there is excellent overlap of the lowest energy quartet ligand field absorption band (Q_1) with the band edge PL of the QDs. This feature suggests that QD → **1** energy transfer via the Förster mechanism would be favorable.[28] In the same context, **2** shows moderate overlap, but **3** shows very little. Static and time-resolved PL studies, as well as fs flash photolysis experiments with time-resolved transient absorbance detection, were all carried out in buffer solution.

QD PL Quenching by *trans*-Cr(cyclam)Cl_2^+. Figure 2A shows the PL behavior of solutions containing a fixed concentration (~190 nM) of QDs and varied concentrations of **1** (0−1000 μM). The PL intensity of the QD decreases with increasing [**1**]. A Stern−Volmer analysis (Figure 2B; I being the intensity at the λ_{max}) exhibits nonlinear behavior with the quenching effect leveling off for [**1**] greater than 500 μM. This behavior is inconsistent with simple diffusional quenching of the optically excited QDs and is indicative of a different type of photophysical interaction between the QD and cyclam complex(es). Pure diffusional quenching should exhibit a linear plot throughout the concentration range according to the Stern−Volmer treatment ($I_0/I = 1 + K_{SV}[Q]$, where $K_{SV} = k_q\tau_0$).[28b] Instead, the plots are nonlinear. Furthermore, if one takes the initial slope of this plot at low [**1**] as K_{SV} and calculates a k_q value by using the lifetime data (see treatment below), the value would be greater than the limiting second-order rate constant for diffusion in aqueous solutions. Thus, instead of invoking a diffusional mechanism for quenching, which, if operational, would be a minor contributor, the discussion below will lead to a model where a nondiffusional process, involving ion pairing between

(25) O'Connor, D. V.; Phillips, D. *Time Correlated Single Photon Counting*; Academic Press: London, 1984.
(26) Klimov, V. I.; McBranch, D. W. *Opt. Lett.* **1998**, *23*, 277−279.
(27) Kutal, C.; Adamson, A. W. *Inorg. Chem.* **1973**, *12*, 1990−1994.
(28) (a) Förster, T. *Discuss. Faraday Soc.* **1959**, *27*, 7−17. (b) Lakowicz, J. R. *Principles of Fluorescence Spectroscopy*, 2nd ed.; Kluwer Academic: New York, 1999.

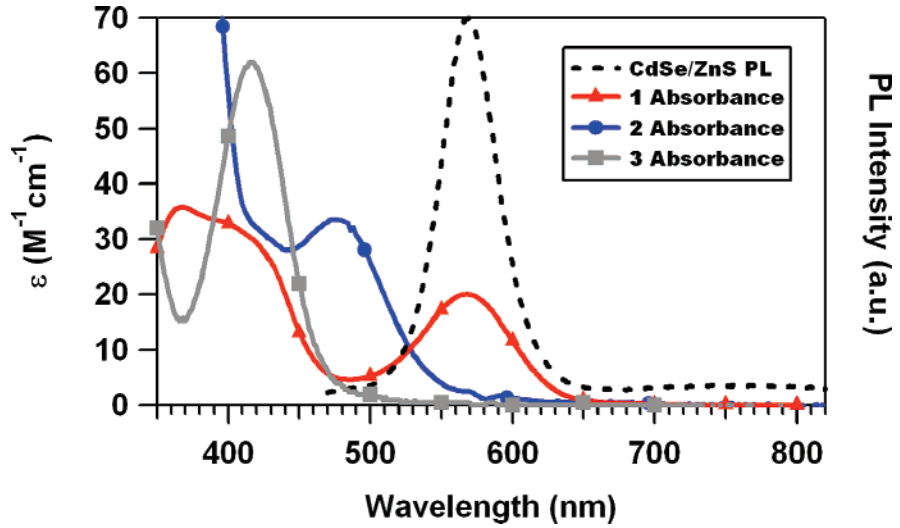

Figure 1. Comparison of the spectral overlap between the QD PL and the absorption spectra of *trans*-Cr(cyclam)Cl_2^+ (**1**, Cl^- salt), *trans*-Cr(cyclam)-$(ONO)_2^+$ (**2**, BF_4^- salt), and *trans*-Cr(cyclam)$(CN)_2^+$ (**3**, ClO_4^- salt). The spectra were recorded in pH 8.2 phosphate buffered (15 mM) solution.

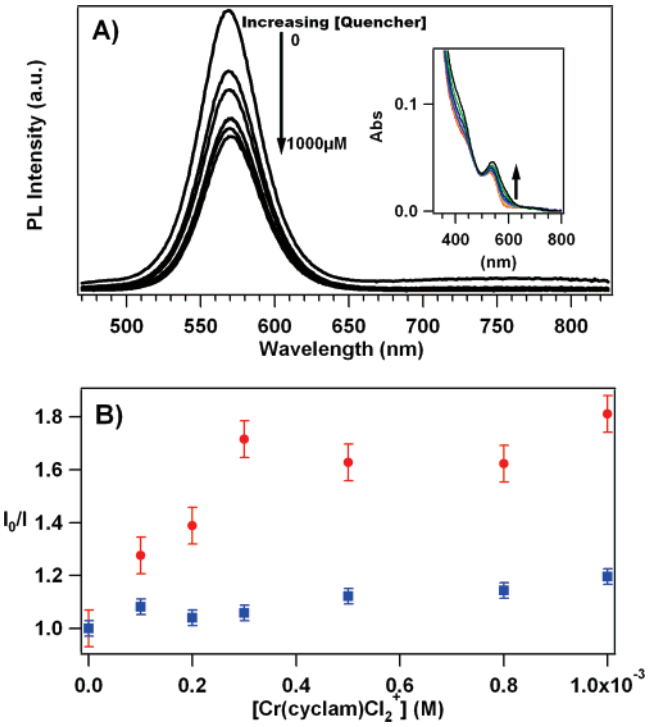

Figure 2. (A) Photoluminescence spectra of the QDs showing changes due to increasing concentration of **1** in pH 8.2 phosphate buffer solution (15 mM). Each trace represents an independently prepared sample having a constant QD concentration (190 nM) and different concentrations of **1** (0−1000 μM). The samples were excited at 460 nm where the absorbance of **1** is negligible at the concentrations used here. (Inset) UV−vis absorbance of each sample. Arrow indicates increasing [**1**]. (B) Stern−Volmer type plot where I is the PL intensity of the QDs at the λ_{max} for various solutions with different concentrations of **1** and I_0 is the PL intensity of the QDs in the absence of **1**. The upper set of points (●) indicate data acquired in 15 mM phosphate buffer solution at pH 8.2, whereas the lower set (■) were acquired under otherwise identical solutions with 250 mM added KCl.

the anionic QD surface and multiple *trans*-Cr(cyclam)Cl_2^+ cations, appears more likely.

If such electrostatic assembly of Cr(III) cations on the QD surfaces is indeed responsible for the quenching, this effect should be attenuated by adding another electrolyte; Figure 2B shows that added KCl (250 mM) strongly reduces the impact of added **1** on the QD PL, presumably by screening the

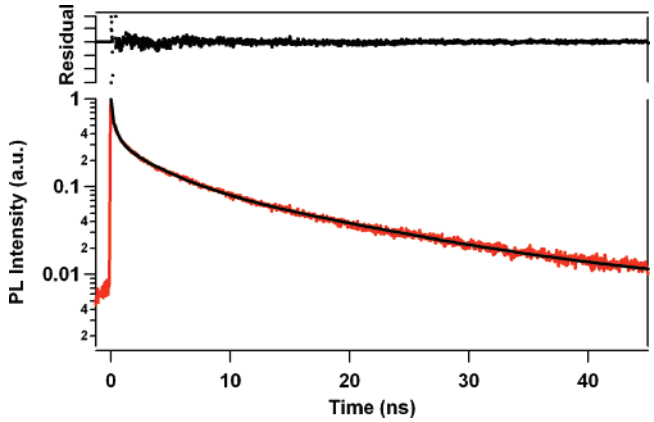

Figure 3. Time-resolved photoluminescence of the water-soluble QDs (190 nM) in aqueous pH 8.2 phosphate buffer solution. QDs were excited with ~120 fs pulses tuned to 460 nm, and the PL was monitored at λ_{max} = 570 nm. The trace through the data represents a fit according to eq 1 with n = 4 (see text). The residual plot above the data demonstrates the "goodness of fit".

electrostatic interaction between the negatively charged QDs and the cationic Cr(III) complex. As a control, it should be noted that, under otherwise analogous conditions, there was little effect of added KCl (up to 1 M) on QD PL intensities in the absence of added **1** (Supporting Information Figure S2).

The complicated time-resolved PL behavior of the QD solutions without added **1** is shown in Figure 3. The PL decay is multiexponential, as is common for such QD systems.[29] An acceptable fit to these data (Figure 3, random noise in the residuals) was obtained using the relationship described in eq 1 with n = 4. The multiexponential luminescence decay kinetics indicate the heterogeneous excited-state behavior of QDs in an ensemble measurement.[30] Although one possibility is that the QDs represent a distribution of sizes, the relatively narrow band shapes of the absorption and emission bands belie this.

(29) (a) Kloepfer, J. A.; Bradforth, S. E.; Nadeau, J. L. *J. Phys. Chem. B* **2005**, *109*, 9996−10003. (b) Selmarten, D.; Jones, M.; Rumbles, G.; Yu, P.; Nedeljkovic, J.; Shaheen, S. *J. Phys. Chem. B* **2005**, *109*, 15927−15932. (c) Crooker, S. A.; Barrick, T.; Hollinsworth, J. A.; Klimov, V. I. *Appl. Phys. Lett.* **2003**, *82*, 2793−2795. (d) Javier, A.; Magana, D.; Jennings, T.; Strouse, G. F. *Appl. Phys. Lett.* **2003**, *83*, 1423−1425.
(30) Klimov, V. I.; McBranch, D. W.; Leatherdale, C. A.; Bawendi, M. G. *Phys. Rev. B* **1999**, *60*, 13740−13749.

$$I(t) = \sum_{i=1}^{n} \alpha_i \exp(-t/\tau_i) \quad (1)$$

Figure 4 shows the effect of added **1** on the temporal PL behavior. Qualitatively, it is seen that the decay is accelerated. Again, these data can be fit to eq 1, and the lifetimes and amplitude so generated are listed in Table 1. In this analysis, the lifetime (τ_1) of the shortest component was limited by the instrument response function (~55 ps) and the amplitude α_1, calculated to be 0.39 in the absence of quencher, was assumed to be invarient. The remaining resolvable components show shorter lifetimes with increasing concentration of **1**, whereas the amplitude of the second component, α_2, increases at the expense of the longest lived component α_4. Notably, quenching of the τ_4 component accounts for over 75% of the total loss in the integrated PL intensity, so any error induced by assuming a constant value of a_1t_1 would be minor.

The steady state and time-resolved PL data demonstrate that added **1** quenches the photoluminescence of the water-soluble CdSe/ZnS core/shell quantum dots in a concentration-dependent manner. As noted above, the initial slope of the plot shown in Figure 2B gives an estimated K_{SV} value of 1950 M^{-1}. If this were assumed to be due to dynamic quenching of the longest lived component of the QD PL, ($\tau_0 = \tau_4 = 15.4$ ns), the estimated k_q (K_{SV}/τ) would be $\sim 1.3 \times 10^{11}$ M^{-1} s^{-1}, an order of magnitude faster than diffusion limits in this medium. Such a high apparent k_q suggests ground-state complex formation between donor and acceptor prior to photoexcitation, that is, a static quenching mechanism rather than dynamic quenching.[31]

One can attribute the quenching to electrostatic assemblies between the anionic QDs and the cationic complexes **1**. Water solubility of the core/shell CdSe/ZnS QDs was accomplished by deprotonation of the dithiol dihydrolipoic acid ligands in the mildly basic medium. From the estimated number of Zn^{2+} centers on the surface,[32] the QDs would accommodate up to 600 DHLA ligands,[33] assuming a ratio of one DHLA per two zinc surface ions. Earlier studies have reported that >85% of surface ligand sites are exchanged during a typical recapping procedure.[33a] Although one might not expect complete ionization of these surface DHLA ligands even at pH 8.2, there is little doubt that the QD surfaces have multiple negative charges and should form electrostatic ion-pairing interactions with a number of the *trans*-Cr(cyclam)Cl_2^+ cations. Accumulation of multiple acceptors at the QD surface provides multiple channels for nonradiative excited-state decay following optical excitation.

PL Quenching by *trans*-Cr(cyclam)$(ONO)_2^+$. The band edge PL of the QDs in buffered solutions was also quenched when progressively higher concentrations of **2** (0−1000 μM) were added (Figure S3, Supporting Information), and a small red-shift of the emission maximum (~3 nm) was observed (Figure S4). This quenching occurs irrespective of the excitation wavelength (366 or 546 nm), although the relative effect appears somewhat stronger for the shorter wavelength.[34] Again we attribute the quenching by **2** to the formation of an electrostatic assembly between multiple units of **2** and the anionic QD surface. The Stern−Volmer type plot of I_0/I vs [**2**] (Supporting Information, Figure S5) is similar to Figure 2B, although there are some quantitative differences, most significantly the quenching being ~20% larger for **2** than for equivalent concentrations of **1**. The effect again levels off at ~500 μM, perhaps due to saturation of the QD hydration sphere with the cationic metal complexes.

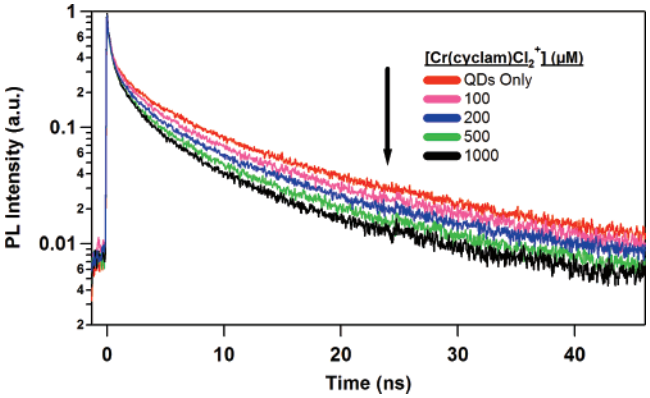

Figure 4. Comparison of time-resolved QD PL as a function of increasing [**1**]. These temporal measurements were made with the samples used to generate the steady-state emission spectra shown in Figure 2.

Table 1. Computed Lifetimes (τ in ns) and Amplitudes ($\Sigma\alpha_i = 1.00$) (using eq 1) for the QD Emission Data with Various Concentrations of *trans*-[Cr(cyclam)Cl_2]Cl Salt[a]

[1] (μM)	α_1	τ_1	α_2	τ_2	α_3	τ_3	α_4	τ_4	$\Sigma\alpha_x\tau_x$	Σ_0/Σ[b]
0	0.39	0.055	0.31	0.500	0.21	3.54	0.12	15.4	2.8	1.00
100		IRF	0.33	0.499	0.20	3.17	0.10	14.1	2.2	1.27
200		IRF	0.35	0.466	0.21	2.85	0.10	13.0	2.1	1.33
300		IRF	0.36	0.454	0.20	2.67	0.09	12.1	1.8	1.56
500		IRF	0.37	0.476	0.20	2.72	0.09	11.4	1.8	1.56
800		IRF	0.36	0.467	0.20	2.38	0.09	9.9	1.6	1.75
1000		IRF	0.36	0.469	0.20	2.30	0.09	9.4	1.5	1.87

[a] Measurement of the fastest detected decay process is limited by the instrument response function (IRF ≈ 55 ps), and the value a_1t_1 is assumed to be constant. [b] $\Sigma_0 = \Sigma\alpha_x\tau_x$ in the absence of **1**. $\Sigma = \Sigma\alpha_x\tau_x$ for various [**1**].

Effect of Added *trans*-[Cr(cyclam)$(CN)_2$]ClO_4. For **3**, the quartet ligand field absorption bands are shifted strongly to the blue with respect to those of **1** and **2**, owing to the much greater ligand field strength of the axial cyano groups (Figure 1). As a consequence, there is virtually no spectral overlap between the Q_1 absorption band of **3** and the QD PL band centered at 570 nm. Thus, it is significant that added **3**, unlike **1** and **2**, does not quench the band-edge PL (Figure S6). For example,

(31) Maurel V.; Laferrière, M.; Billone, P.; Godin, R.; Scaiano, J. C. *J. Phys. Chem. B* **2006**, *110*, 16353−16358.
(32) The number of Zn atoms on the surface (outermost monolayer of ZnS) was estimated based on the known bulk lattice parameters of ZnS assuming a spherical shell.
(33) (a) Bowen Katari, J. E.; Colvin, V. L.; Alivisatos, A. P. *J. Phys. Chem.* **1994**, *98*, 4109−4117. (b) Becerra, L. R.; Murray, C. B.; Griffin, R. G.; Bawendi, M. G. *J. Chem. Phys.* **1994**, *100*, 3297−3300.
(34) (a) It should be noted that in the former case, the samples were studied under air atmosphere to approximate the conditions used during the photochemical experiments. At this point it is unclear what effect air (presumably O_2) has on the PL of these particular QDs. It has been shown in this laboratory[34b] and by others (see for example: (i) Nazzal, A. Y.; Wang, X.; Qu, L.; Yu, W.; Wang, Y.; Peng, X.; Xiao, M. *J. Phys. Chem. B* **2004**, *108*, 5507−5515. (ii) Wang, Y.; Tang, Z.; Correa-Duarte, M. A.; Pastoriza-Santos, I.; Giersig, M.; Kotov, N. A.; Liz-Marzán, L. M. *J. Phys. Chem. B.* **2004**, *108*, 15461−15469. (iii) Myung, N.; Bae, Y.; Bard, A. J. *Nano Lett.* **2003**, *3*, 747−749.) that various QD preparations (solution and solid state) undergo changes in PL spectral position and intensity as a function of extended light irradiation in the presence of O_2. Although similar changes are not expected under the low light intensities used for the present experiment, the influence of dioxygen on the PL behavior of the current system has not been systematically evaluated. (b) Neuman, D. Ph.D. Dissertation, University of California, Santa Barbara 2007.

solutions containing ~210 nM QDs and up to 500 μM **3** show only slight variations in the band edge PL (<10%) from solutions with no quencher present.

In addition to the very prominent band edge emission, the PL spectrum of the water-soluble QDs also shows a weak broad band centered at ~750 nm of the type that has been attributed[35] to emission from a surface "trap" state. It is notable that this trap emission is largely depleted by even the lowest concentration (100 μM) of **1** utilized in the steady-state quenching experiments (Figure 2). Similar depletion of this feature was also seen (Figure S6) for the lower concentrations of **2** and **3** used to study the effects of the various Cr(III) complexes on the QD PL.

FRET Mechanism for PL Quenching. Given the spectral overlap between the QD PL and the Q_1 absorbance bands of **1** and **2** and the absence of such overlap with **3** (Figure 1), quenching by the first two but not the third suggests the operation of Förster resonance energy transfer (FRET) as the likely quenching mechanism. The FRET formalism has been used to describe the nonradiative energy transfer from QDs to various acceptors, including other QDs, quantum wires, dye molecules, and metalloproteins.[36−38] In this framework, the predicted rate constant for energy transfer (k_{EN}) from the donor chromophore (D) to a single acceptor chromophore (A) is given by[28]

$$k_{EN}(r) = \frac{\Phi_{PL}\kappa^2}{\tau_{D(0)}r^6}\left(\frac{9000(\ln 10)}{128\pi^5 N n^4}\right)J(\lambda) = \frac{1}{\tau_{D(0)}}\left(\frac{R_0}{r}\right)^6 \qquad (2)$$

where Φ_{PL} is the PL donor quantum yield in the absence of acceptor, $\tau_{D(0)}$ is the donor lifetime in the absence of acceptor, κ is the dipole−dipole orientation factor ($\kappa^2 = 2/3$ for randomly oriented dipoles), N is Avogadro's number, and n is the refractive index of the medium. $J(\lambda)$ takes into account the spectral overlap between the donor PL and the acceptor absorption spectra as a function of the wavelength λ. The Förster radius R_0 represents the D−A separation distance where the rate of energy transfer, k_{EN}, and the rate of excited-state deactivation of D ($1/\tau_{D(0)}$) are equal. By using the spectral data of Figure 1 to calculate $J(\lambda)$, one obtains a value for $R_0 = 2.8$ nm for the quenching of QDs by the Cr cyclam complex, if we assume a $\Phi_{PL} = 0.02$ and $\tau_{D(0)} = 15.4$ ns (i.e., τ_4). (Details of this calculation are described in the Supporting Information.)

To apply the FRET formalism in the current study, the D−A distance r needs to be estimated. The QD core radius R_{core} would be 1.9 nm (spherical shape assumed). To this is added the thickness of the ZnS shell (~6 × 0.31 nm/ZnS monolayer = 1.9 nm)[18] and of the DHLA surface layer (~1 nm) to give an overall radius R_{C+S+L} of 4.8 nm (Figure 5). This can be compared to the reported hydrodynamic radii of 6−7 nm for similar water-soluble core/shell/ligand CdSe/ZnS/DHLA QDs (λ_{em} = 570 nm) as determined by dynamic light scattering measurements.[39] One may assume that the electrostatic assembly process draws the Cr(cyclam)Cl_2^+ cations into the hydration sphere as conceptualized by Figure 5, so a distance of ~5 nm from the center of the core or of ~3 nm from the core surface would be a reasonable estimate.

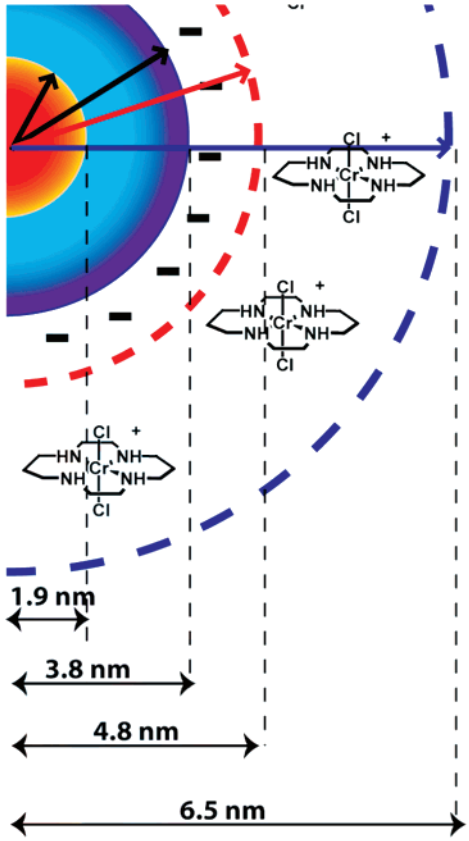

Figure 5. Idealized drawing of *trans*-Cr(cyclam)Cl_2^+ cations electrostatically assembled in the hydration sphere of DHLA coated CdSe/ZnS core/shell QD. The radius was estimated from measurements of similar systems.[39]

Both the center[37] and the surface[40] have been used by others to estimate distances for FRET in QD systems. If one uses the former, eq 2 would give a calculated k_{EN} in the range (0.42−2.6) × 10^6 s^{-1} for a single Cr(cyclam)Cl_2^+ cation lying within the hydration sphere (~6.5 > r > 4.8 nm). (The longest lifetime τ_4 was used for this estimate, because changes in this PL decay component account for 75% of the emission yield decrease upon addition of **1**.) On the other hand, if the distance from the core surface were used (~4.6 > r > 2.9 nm), the estimated k_{EN} values would be higher, (0.34−5.4) × 10^7 s^{-1}. Even these latter values would be too small to account for the quenching effect on the longest PL lifetimes by a single Cr(cyclam)Cl_2^+ cation. However, it is important to reemphasize that the large QD surface area can accommodate numerous acceptors. Thus, even an r value based on the core center might be reasonable if there is linear enhancement of the quenching kinetics due to the multiple acceptors.[37] This model is represented by eq 3, where

(35) Klimov, V. I., Ed. *Semiconductor and Metal Nanocrystals-Synthesis and Electronic and Optical Properties*; Marcel Dekker: New York, 2004.
(36) (a) Kagan, C. R.; Murray, C. B.; Bawendi, M. G. *Phys. Rev. B* **1996**, *54*, 8633−8643. (b) Crooker, S. A.; Hollingsworth, J. A.; Tretiak, S.; Klimov, V. I. *Phys. Rev. Lett.* **2002**, *89*, 186802-1−4. (c) Achermann, M.; Petruska, M. A.; Crooker, S. A.; Klimov, V. I. *J. Phys. Chem. B* **2003**, *107*, 13782−13787. (d) Lee, J.; Govorov, A. O.; Kotov, N. A. *Nano Lett.* **2005**, *5*, 2063−2069. (e) Wargnier, R.; Baranov, A. V.; Maslov, V. G.; Stsiapura, V.; Artemyev, M.; Pluot, M.; Sukhanova, A.; Nabiev, I. *Nano Lett.* **2004**, *4*, 451−457.
(37) (a) Clapp, A. R.; Medintz, I. L.; Mattoussi, H. *Chem. Phys. Chem.* **2006**, *7*, 47−57 and references therein. (b) Clapp, A. R.; Medintz, I. L.; Mauro, J. M.; Fisher, B. R.; Bawendi, M. G.; Mattoussi, H. *J. Am. Chem. Soc.* **2004**, *126*, 301−310.
(38) Ipe, B. I.; Niemeyer, C. M. *Angew. Chem., Int. Ed.* **2006**, *45*, 504−507.
(39) (a) Pons, T.; Medintz, I. L.; Mattoussi, H. *Proc. SPIE* **2006**, *6096*, 60961H-1−10. (b) Ipe, B. I.; Shukla, A.; Lu, H.; Zou, B.; Rehage, H.; Niemeyer, C. M. *Chem. Phys. Chem.* **2006**, *7*, 1112−1118.
(40) Dayal, S.; Królicki, R.; Lou, Y.; Qiu, X.; Berlin, J. C.; Kenney, M. E.; Burda, C. *Appl. Phys. B* **2006**, *84*, 309−315.

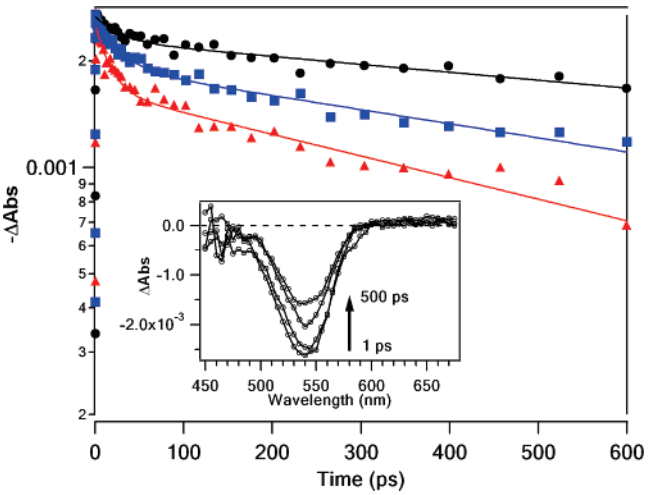

Figure 6. TA dynamics of the QDs measured at 530 nm for 1.9 μM solutions of QDs with varied concentrations of **1**. The data sets are 0 mM (●), 5 mM (■), and 10 mM (▲) **1**. The lines represent double exponential fits to the data. (Inset) Spectral data for the recovery of the bleach of the QD 1S transition (*without* **1** added) at various delay times after the pump pulse.

τ is the measured lifetime in the presence of the quencher and the term N_q accounts for the number of acceptors intimately associated with the QD.

$$\tau^{-1} = \tau_{D(0)}{}^{-1} + N_q k_{EN} \qquad (3)$$

The decrease in τ_4 seen for the highest [1] (Table 1) would require $N \approx 18$ for the k_{EN} calculated for $r = 4.8$ nm and $N \approx 110$ for that calculated for $r = 6.5$ nm. The latter number is close to the capacity for Cr(cyclam)Cl_2^+ cations in the QD hydration sphere.[17,41]

It is unclear why **2** is at least as effective a quencher as **1** given the former's lower spectral overlap of its Q1 band with the CdSe/ZnS PL (Figure 1). One possible explanation lies in the strong distance dependence of the rate of FRET ($k_{EN} \propto 1/r^6$) and, thus, its overall efficiency, predicted by eq 2. Even small differences in the average donor/acceptor distance for assemblies of QDs with **1** versus **2** may have large effects on the observed PL quenching efficiency. Notably, we also observed quenching of the QD PL lifetime with added **2** in analogy to that seen for mixtures with **1**, that is, shortening of the longer decay components with a modest enhancement in the contribution of τ_2 (Table S1, Supporting Information). This observation suggests that the nonzero spectral overlap of QD PL with the ligand field absorption band of **2** facilitates quenching by a similar pathway, namely via energy transfer.

Transient Absorbance Experiments. Figure 6 displays the TA behavior initiated by fs flash photolysis of QD solutions (1.9 μM) in the presence of different concentrations of **1** (0, 5, 10 mM). Prompt transient bleaching of the band edge transition was observed and the decay of this bleach displayed several components. A fast process with a time constant of ~20−30 ps accounts for roughly 15% of the total signal for [**1**] = 0. The remaining decay observable within the instrumentation limits demonstrated a time constant of ~1−2 ns. (The dynamics of the substantial residual bleach at the end of the latter time frame were not accessed by this experiment.) Introduction of **1** diminished the longer component of the decay, which was manifested in an increase of the relative amplitude of the fast process to 35% at the highest quencher/QD ratio (Table S2, see Supporting Information). These data suggest that **1** introduces a new, very fast, excited decay pathway in the QDs. The residual bleach was also significantly decreased by added **1**, and this observation is consistent with the quenching of the longer lived PL components noted in Table 1.

QD preparations are known to include "bright" and "dark" species;[42] the former display the band-edge PL whereas the latter do not, owing to efficient charge carrier trapping. The ultrafast TA experiment probes a time scale not accessible in the time-resolved PL data and samples the entire ensemble, whereas PL only samples QDs that decay with a measurable luminescence. Decay of the 1S bleach on the subnanosecond time scale has been associated with surface trapping of charge carriers for a portion of the QDs,[30] and in the present case, it appears that **1** introduces a new component, or enhances an existing one, associated with this process. Although the increased contribution to the very short-lived TA decay appears to be outside the expectation of a FRET mechanism, a recent study has demonstrated bleach dynamics effects on a similar time scale (~30−50 ps) for the interaction of pthalocyanines (Pcs) with CdSe QDs.[40,43]

One might postulate that the effects seen in the short time regime of the TA experiment is associated with the surface-trapped carriers that give rise to the weak broad luminescence band at ~750 nm, which is quenched by low concentrations (100 μM) of **1**. Similar effects are seen for added **2** and **3**, despite failure by the latter to quench the band edge emission band. Charge transfer between the trapped carrier(s) and complex at or near the QD surface would be consistent both with quenching of the deep trap luminescence and with acceleration of the bleach dynamics observed in the TA experiment. In this context we propose that while energy transfer is the dominant mechanism for the band edge PL quenching by **1** or **2**, another process is active whereby the deep trap luminescence is quenched, perhaps due to ultrafast charge transfer between the QD and surface-associated complex cations.

The latter conclusion is further supported by comparison of the reduction potentials of the Cr complexes and the QDs. As shown in Figure 7, the $Cr^{IV/III}$ redox couple of each complex lies above the valence band potential of the QDs but below that of the conduction band. This characteristic would make hole injection from optically excited QD (from a shallow trap state) to the surface associated Cr(III) complex energetically feasible. Such hole transfer would quench the low-energy emission from such states.

Photosensitized NO Release from *trans*-Cr(cyclam)-$(ONO)_2^+$. The quenching of QD PL by **2** was also accompanied

(41) (a) Cebula, J.; Ottewill, R. H.; Ralston, J.; Pusey, P. N. *J. Chem. Soc., Faraday Trans.* **1981**, *I77*, 2585−2612. (b) Pompa, P. P.; Chiuri, R.; Manna, L.; Pellegrino, T.; del Mercato, L. L.; Parak, W. J.; Calabi, F.; Cingolani, R.; Rinaldi, R. *Chem. Phys. Lett.* **2006**, *417*, 351−357.

(42) Ebenstein, Y.; Maokari, T.; Banin, U. *Appl. Phys. Lett.* **2002**, *80*, 4033−4035.

(43) Dayal, S.; Lou, Y.; Cristina, A.; Samia, S.; Berlin, J. C.; Kenney, M. E.; Burda, C. *J. Am. Chem. Soc.* **2006**, *128*, 13974−13975.

(44) Sykora, M.; Petruska, M. A.; Alstrum-Acevedo, J.; Bezel, I.; Meyer, T. J.; Klimov, V. I. *J. Am. Chem. Soc.* **2006**, *128*, 9984−9985.

(45) As a reviewer has pointed out, flocculation of the QDs might be expected as the result of charge neutralization of the surface owing to the ion pairing with the cationic Cr(III) complexes. Such flocculation was indeed observed to occur very slowly upon standing for solutions at the highest quencher concentrations used. For this reason, photophysics measurements were only made with freshly prepared buffer solutions that did not indicate formation of insoluble particles.

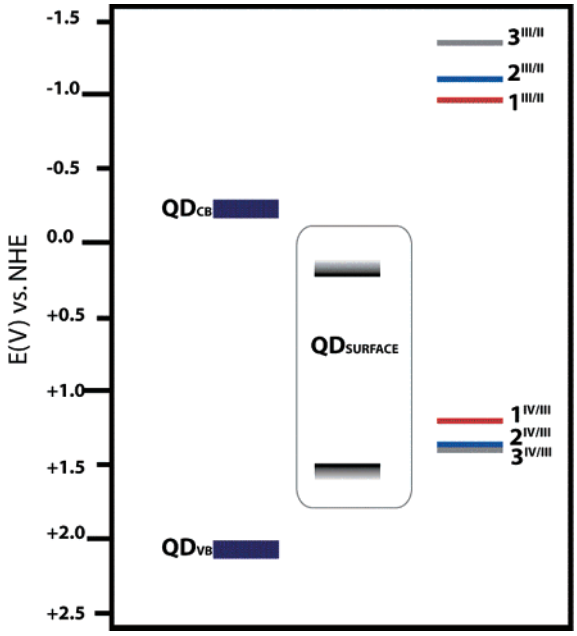

Figure 7. Energy level diagram showing relative positions of the QD valence and conduction bands (see ref 45) and the reduction potentials from Cr^{III} to Cr^{II} and Cr^{IV} to Cr^{III} for the ground state chromium complexes as measured by cyclic voltammetry.

Scheme 1

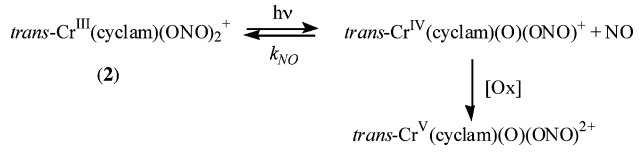

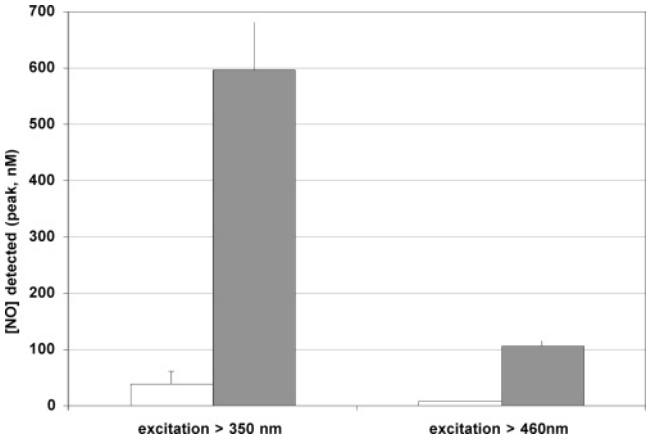

Figure 8. Comparison of the NO detected (normalized signal) after irradiation of solutions containing **2** (200 μM in phosphate buffer pH 8.2) without (white) and with (gray) QDs (200 nM).

by sensitization of the photoreaction illustrated by Scheme 1, as described in an earlier communication from this laboratory.[15] The release of NO from **2** can be initiated by direct photolysis of its weakly absorbing, visible range LF bands as illustrated in Figure 8 for 200 μM solutions of **2** in pH 8.2 buffer. However, when the water-soluble CdSe/ZnS core/shell QDs (200 nM) were added, NO generation was dramatically enhanced (Figure 8). This can be attributed to energy transfer from the excited QDs to *trans*-Cr(cyclam)$(ONO)_2^+$ cations electrostatically bound to the surface.

The marked enhancement of the photochemical activity of **2** induced by adding QDs to the solution is similar regardless of whether the excitation with the mercury arc lamp used a filter that cut off wavelengths <350 nm or one that cut off wavelengths <460 nm. In both cases, ~15-fold enhancement in NO release is seen from the assemblies of QDs and **2** (the smaller absolute production of NO in the latter case is due to the lower intensity of light absorbed). This marked increase indicates that the quantum dots are acting as antennae, increasing the amount of light absorbed by **2** and thus the NO released, much the same as pendant chromophores have been used to stimulate photochemical NO release from analogs of **2**.[3c,d] On the basis of these results, quantum dot constructs offer an interesting new approach for the design of photochemical drugs for the release of NO, as well as other bioactive agents, from an appropriate precursor.

Summary

The PL quenching behavior of the water-soluble QDs in response to added **1** or **2** is consistent with an energy-transfer mechanism involving electrostatic assemblies of these Cr(III) cations on the anionic quantum dot surfaces. The quenching of the emissive QDs was analyzed in terms of a FRET mechanism and could be attributed to the presence of a number of Cr(III) cations within the QD hydration sphere. The FRET analysis is consistent with the leveling of the PL quenching effect, owing to saturation of the QD surfaces with **1** or **2**, as estimated by independent calculations based on steric effects.

This system confirms that QDs can function as effective sensitizers to photochemical reactions of transition metal complexes, notably NO release from **2**, and clearly exemplifies the enhanced energy-transfer efficiency when there are multiple acceptors associated with the donor. Due to the strong absorbance of the QDs, photoinduced release of NO from the assemblies containing **2** is strongly enhanced at visible wavelengths. We are currently in the process of quantifying QD sensitized release of NO from **2** and from other photochemical NO precursors after single or two photon excitation. Meanwhile, studies are ongoing to develop more sophisticated QD/NO donor platforms in which derivatives of **2** or other NO donor compounds are strongly associated with the QD sensitizers via covalent surface attachment. We envision that such systems will present a new class of photochemical prodrugs for delivery of NO on demand.

Acknowledgment. These studies were supported by a grant to P.C.F. from the National Science Foundation (CHE-0352650), to G.F.S. from the National Institute of Health (NBIB 7 R01 EB000832), and by a UC-CARE grant from Los Alamos National Laboratory to P.C.F. and G.F.S. We thank Prof. Steve Buratto and Dr. Hedi Mattoussi for helpful discussions.

Supporting Information Available: Figures S1−S6 display the optical properties of the QDs under various conditions discussed in the text. More detailed discussions of the methods used to prepare QDs and to determine the Förster radius, the energy-transfer rate, and the number of chromium complexes that can associate around a single QD are also presented. This material is available free of charge via the Internet at http://pubs.acs.org.

JA074164S